Inferring the effective start dates of non-pharmaceutical interventions during COVID-19 outbreaks

Ilia Kohanovski[a], Uri Obolski[b,c], and Yoav Ram[a,*]

[a]School of Computer Science, Interdisciplinary Center Herzliya, Herzliya 4610101, Israel
[b]School of Public Health, Tel Aviv University, Tel Aviv 6997801, Israel
[c]Porter School of the Environment and Earth Sciences, Tel Aviv University, Tel Aviv 6997801, Israel
[*]Corresponding author: yoav@yoavram.com

May 19, 2020

Abstract

During February and March 2020, several countries implemented non-pharmaceutical interventions, such as school closures and lockdowns, with variable schedules to control the COVID--19 pandemic caused by the SARA-CoV-2 virus. Overall, these interventions seem to have successfully reduced the spread of the pandemic. We hypothesize that the official and effective start date of such interventions can significantly differ, for example due to slow diffusion of guidelines in the population, or due to unpreparedness of the authorities and the public. We use an SEIR epidemiological model and an MCMC inference framework to estimate the effective start of NPIs in several countries, and compare this effective dates to the official dates. We report our finding of both late and early effects of NPIs, and discuss potential causes and consequences of our results.

Introduction

The COVID-19 pandemic has resulted in implementation of extreme non-pharmaceutical interventions (NPIs) in many affected countries. These interventions, from social distancing to lockdowns, are applied in a rapid and widespread fashion. The NPIs are designed and assessed using epidemiological models, which follow the dynamics of the viral infection to forecast the effect of different mitigation and suppression strategies on the levels of infection, hospitalization, and fatality. These epidemiological models usually assume that the effect of NPIs on disease transmission begins at the officially declared date (e.g. Flaxman et al.[6], Gatto et al.[8], Li et al.[11]).

Adoption of public health recommendations is often critical for effective response to infectious diseases, and has been studied in the context of HIV[10] and vaccination[4,16], for example. However, behavioral and social change does not occur immediately, but rather requires time to diffuse in the population through media, social networks, and social interactions. Moreover, compliance to NPIs may differ between different interventions and between people. For example, in a survey of 2,108 adults in the UK during Mar 2020, Atchison et al.[2] found that those over 70 years old were more likely to adopt social distancing than young adults (18-34 years old), and that those with lower income were less likely to be able to work from home and to self-isolate. Similarly, compliance to NPIs may be impacted by personal experiences. Smith et al.[13] have surveyed 6,149 UK adults in late April and found that people who believe they have already had COVID-19 are more likely to think they are immune, and less likely to comply with social distancing measures. Compliance may also depend on risk perception as perceived by the the number of domestic cases or even by reported cases in other regions and countries. Interestingly, the perceived risk of COVID-19 infection has likely caused a reduction in the number of influenza-like illness cases in the US starting from mid-February[17].

Here, we hypothesize that there is a significant difference between the official start of NPIs and their adoption by the public and therefore their effect on transmission dynamics. We use a *Susceptible-Exposed-Infected-Recovered* (SEIR) epidemiological model and *Markov Chain Monte Carlo* (MCMC) parameter estimation framework to estimate the effective start date of NPIs from publicly available COVID-19 case data in several geographical regions. We compare these estimates to the official dates and find both late and early effects of NPIs on COVID-19 transmission dynamics. We conclude by demonstrating how differences between the official and effective start of NPIs can confuse assessments of the effectiveness of the NPIs in a simple epidemic control framework.

Models and Methods

Data. We use daily confirmed case data $\mathbf{X} = (X_1, \ldots, X_T)$ from several different countries. These incidence data summarize the number of individuals X_t tested positive for SARS-CoV-2 RNA (using RT-qPCR) at each day t. Data for Wuhan, China retrieved from Pei and Shaman[12], data for 11 European countries retrieved from Flaxman et al.[6]. Regions in which there were multiple sequences of days with zero confirmed cases (e.g. France), we cropped the data to begin with the last sequence so that our analysis focuses on the first sustained outbreak rather than isolated imported cases. For dates of official NPI dates see Table 1.

SEIR model. We model SARS-CoV-2 infection dynamics by following the number of susceptible S, exposed E, reported infected I_r, and unreported infected I_u individuals in a population of size N. This model distinguishes between reported and unreported infected individuals: the reported infected are those that have enough symptoms to eventually be tested and thus appear in daily case reports, to which we fit the model.

Country	First	Last
Austria	Mar 10 2020	Mar 16 2020
Belgium	Mar 12 2020	Mar 18 2020
Denmark	Mar 12 2020	Mar 18 2020
France	Mar 13 2020	Mar 17 2020
Germany	Mar 12 2020	Mar 22 2020
Italy	Mar 5 2020	Mar 11 2020
Norway	Mar 12 2020	Mar 24 2020
Spain	Mar 9 2020	Mar 14 2020
Sweden	Mar 12 2020	Mar 18 2020
Switzerland	Mar 13 2020	Mar 20 2020
United Kingdom	Mar 16 2020	Mar 24 2020
Wuhan	Jan 23 2020	Jan 23 2020

Table 1: Official start of non-pharmaceutical interventions. The date of the first intervention is for a ban of public events, or encouragement of social distancing, or for school closures. In all countries except Sweden, the date of the last intervention is for a lockdown. In Sweden, where a lockdown was not ordered during the studied dates, the last date is for school closures. Dates for European countries from Flaxman et al.[6], date for Wuhan, China from Pei and Shaman[12]. See Figure S2 for a visual presentation.

Susceptible (S) individuals become exposed due to contact with reported or unreported infected individuals (I_r or I_u) at a rate β_t or $\mu\beta_t$. The parameter $0 < \mu < 1$ represents the decreased transmission rate from unreported infected individuals, who are often subclinical or even asymptomatic. The transmission rate $\beta_t \geq 0$ may change over time t due to behavioral changes of both susceptible and infected individuals. Exposed individuals, after an average incubation period of Z days, become reported infected with probability α_t or unreported infected with probability $(1 - \alpha_t)$. The reporting rate $0 < \alpha_t < 1$ may also change over time due to changes in human behavior. Infected individuals remain infectious for an average period of D days, after which they either recover, or becomes ill enough to be quarantined. They therefore no longer infect other individuals, and the model does not track their frequency. The model is described by the following equations:

$$\begin{aligned}
\frac{dS}{dt} &= -\beta_t S\frac{I_r}{N} - \mu\beta_t S\frac{I_u}{N} \\
\frac{dE}{dt} &= \beta_t S\frac{I_r}{N} + \mu\beta_t S\frac{I_u}{N} - \frac{E}{Z} \\
\frac{dI_r}{dt} &= \alpha_t\frac{E}{Z} - \frac{I_r}{D} \\
\frac{dI_u}{dt} &= (1-\alpha_t)\frac{E}{Z} - \frac{I_r}{D}.
\end{aligned} \tag{1}$$

The initial numbers of exposed $E(0)$ and unreported infected $I_u(0)$ are considered model parameters, whereas the initial number of reported infected is assumed to be zero $I_r(0) = 0$, and the number of susceptible is $S(0) = N - E(0) - I_u(0)$. This model is inspired by Li et al.[11] and Pei and Shaman[12], who used a similar model with multiple regions and constant transmission β and reporting rate α to infer COVID-19 dynamics in China and the continental US, respectively.

Likelihood function. For a given vector θ of model parameters the *expected* cumulative number of reported infected individuals (I_r) until day t is, following Eq. (1),

$$Y_t(\theta) = \int_0^t \alpha_s \frac{E(s)}{Z}\, ds, \quad Y_0 = 0. \tag{2}$$

We assume that reported infected individuals are confirmed and therefore observed in the daily case report of day t with probability p_t (note that an individual can only be observed once, and that p_t may change over time, but t is a specific date rather than the time elapsed since the individual was infected). We denote by X_t the number of confirmed cases in day t, and by $\tilde{X}_t$ the cumulative number of confirmed cases until day t,

$$\tilde{X}_t = \sum_{i=1}^{t} X_i. \tag{3}$$

Therefore, at day t the number of reported infected yet-to-be confirmed individuals is $(Y_t(\theta) - \tilde{X}_{t-1})$. We therefore assume that X_t conditioned on $\tilde{X}_{t-1}$ is Poisson distributed,

$$\begin{aligned} \Big(X_1 \mid \theta\Big) &\sim Poi\big(Y_1(\theta) \cdot p_1\big), \\ \Big(X_t \mid \tilde{X}_{t-1}, \theta\Big) &\sim Poi\Big(\big(Y_t(\theta) - \tilde{X}_{t-1}\big) \cdot p_t\Big), \quad t > 1. \end{aligned} \tag{4}$$

Hence, the *likelihood function* $\mathbb{L}(\theta \mid \mathbf{X})$ for the parameter vector θ given the confirmed case data $\mathbf{X} = (X_1, \ldots, X_T)$ is defined by the probability to observe $\mathbf{X}$ given θ,

$$\mathbb{L}(\theta \mid \mathbf{X}) = P(\mathbf{X} \mid \theta) = P(X_1 \mid \theta) \cdot P(X_2 \mid \tilde{X}_1, \theta) \cdots P(X_T \mid \tilde{X}_{T-1}, \theta). \tag{5}$$

NPI model. To model non-pharmaceutical interventions (NPIs), we set the beginning of the NPIs to day τ and define

$$\beta_t = \begin{cases} \beta, & t < \tau \\ \beta\lambda, & t \geq \tau \end{cases}, \quad \alpha_t = \begin{cases} \alpha_1, & t < \tau \\ \alpha_2, & t \geq \tau \end{cases}, \quad p_t = \begin{cases} 1/9, & t < \tau \\ 1/6, & t \geq \tau \end{cases}, \tag{6}$$

where $0 < \lambda < 1$. The values for p_t follow Li et al.[11], who estimated the average time between infection and reporting in Wuhan, China, at 9 days before the start of NPIs and 6 days after start of NPIs.

Parameter estimation. To estimate the model parameters from the daily case data $\mathbf{X}$, we apply a Bayesian inference approach. We start our model Δt days[8] before the outbreak (defined as consecutive days with increasing confirmed cases) in each country. The model in Eq. (1) is parameterized by the vector θ, where

$$\theta = \Big(Z, D, \mu, \{\beta_t\}, \{\alpha_t\}, \{p_t\}, E(0), I_u(0), \tau, \Delta t\Big). \tag{7}$$

The likelihood function is defined in Eq. (5). The posterior distribution of the model parameters $P(\theta \mid \mathbf{X})$ is estimated using an *affine-invariant ensemble sampler for Markov chain Monte Carlo* (MCMC)[9] implemented in the `emcee` Python package[7].

We defined the following prior distributions on the model parameters $P(\theta)$:

$$\begin{aligned} Z &\sim Uniform(2,5) \\ D &\sim Uniform(2,5) \\ \mu &\sim Uniform(0.2,1) \\ \beta &\sim Uniform(0.8,1.5) \\ \lambda &\sim Uniform(0,1) \\ \alpha_1,\alpha_2 &\sim Uniform(0.02,1) \\ E(0) &\sim Uniform(0,3000) \\ I_u(0) &\sim Uniform(0,3000) \\ \Delta t &\sim Uniform(1,5) \\ \tau &\sim TruncatedNormal\Big(\frac{\tau^*+\tau^0}{2},\frac{\tau^*-\tau^0}{2},1,T-2\Big), \end{aligned} \tag{8}$$

where the prior for τ is a truncated normal distribution shaped so that the date of the first and last NPI, τ^0 and τ^* (Table 1), are at minus and plus one standard deviation, and taking values only between 1 and $T-2$, where T is the number of days in the data $\mathbf{X}$. We have also tested an uninformative uniform prior $U(1,T-2)$. The uninformative prior could result in non-negligible posterior probability for unreasonable τ values, such as Mar 1 in the United Kingdom. This was probably due to MCMC chains being stuck in low posterior regions of the parameter space. We therefore decided to use the more informative truncated normal prior. Other priors follow Li et al. [11], with the following exceptions. λ is used to ensure transmission rates are lower after the start of the NPIs ($\lambda < 1$). We checked values of Δt larger than five days and found they generally produce lower likelihood, higher DIC (see below), and unreasonable parameter estimates, and therefore chose $U(1,5)$ as the prior.

Model selection. We perform model selection using DIC (deviance information criterion)[14],

$$\begin{aligned} DIC(\theta,\mathbf{X}) &= 2\mathbb{E}[D(\theta)] - D(\mathbb{E}[\theta]) \\ &= 2\log\mathcal{L}(\mathbb{E}[\theta]\mid\mathbf{X}) - 4\mathbb{E}[\log\mathcal{L}(\theta\mid\mathbf{X})], \end{aligned} \tag{9}$$

where $D(\theta) = -2\log\mathcal{L}(\theta\mid\mathbf{X})$ is the Bayesian deviance, and expectations $\mathbb{E}[\cdot]$ are taken over the posterior distribution $P(\theta\mid\mathbf{X})$. We compare models by reporting their relative DIC; lower is better.

Source code. We use Python 3 with the NumPy, Matplotlib, SciPy, Pandas, Seaborn, and emcee packages. All source code will be publicly available under a permissive open-source license at github.com/yoavram-lab/EffectiveNPI. Files containing samples from the posterior distributions will be deposited on FigShare.

Results

Several studies have described the effects of non-pharmaceutical interventions in different geographical regions[6,8,11]. These studies have assumed that the parameters of the epidemiological model change at a specific date, as in Eq. (6), and set the change date τ to the official NPI date τ^* (Table 1). They then fit the model once for time $t < \tau^*$ and once for time $t \geq \tau^*$. For example, Li et al. [11] estimate the dynamics in China before and after τ^* at Jan 23. Thereby, they effectively estimate (β,α_1) and (λ,α_2) separately. Here we estimate the posterior distribution $P(\tau\mid\mathbf{X})$ of the *effective* start date of the NPIs by jointly estimating $\tau,\beta,\lambda,\alpha_1,\alpha_2$ on the entire data per region (e.g. Italy, Austria), rather than

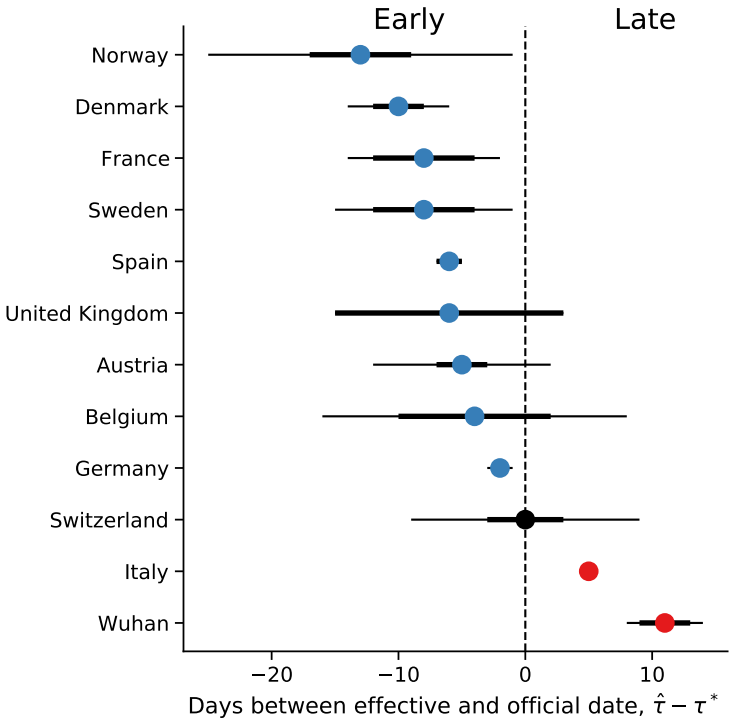

Figure 1: Official and effective start of non-pharmaceutical interventions. The difference between $\hat{\tau}$ the effective and τ^* the official start of NPI is shown for different regions. The effective NPI dates in Italy and Wuhan are significantly delayed compared to the official dates, whereas in Denmark, France, Spain, and Germany, the effective date is earlier than the official date. $\hat{\tau}$ is the posterior median, see Table 2. τ^* is the last NPI date, see Table 1. Thin and bold lines show 95% and 75% credible intervals (area in which $P(|\tau - \hat{\tau}| \mid \mathbf{X}) = 0.95$ and 0.75.)

splitting the data at τ^*. We then estimate the posterior probability $P(\tau \mid \mathbf{X})$ by marginalizing the joint posterior, and estimate $\hat{\tau}$ as the posterior median.

We find that a model that considers an NPI (Eq. (6)) is a better fit to the data than a model without an NPI, i.e. with constant β and α (???.) We compare the official τ^* and effective $\hat{\tau}$ start of NPIs and find that in most regions the effective start of NPI significantly differs from the official date (Figure 1). Indeed, the credible interval on $\hat{\tau}$ does not include τ^* (Figure 1). Moreover, we compared the posterior predictive plots of a model with a free τ with those of a model with τ fixed at τ^*. The model with free τ clearly produces better and less variable predictions (Figure S11).

In the following, we describe our findings on late and early effective start of NPI in detail.

Country	τ^*	τ	75% CI	95% CI	DIC using	Z	D	μ	β	α_1	λ	α_2	$E(0)$	$I_u(0)$	Δt
Austria	Mar 16	Mar 11	2.0	7.0	29.62	3.92	3.59	0.43	1.10	0.06	0.73	0.45	464.24	555.98	2.0
Belgium	Mar 18	Mar 14	6.0	12.0	1.61	3.95	3.56	0.43	1.09	0.22	0.84	0.43	364.73	464.54	2.0
Denmark	Mar 18	Mar 08	2.0	4.0	10.23	3.96	3.47	0.37	1.06	0.04	0.32	0.53	501.86	638.74	2.0
France	Mar 17	Mar 09	4.0	6.0	-456.41	4.00	3.70	0.56	1.14	0.20	0.66	0.45	530.90	607.66	1.0
Germany	Mar 22	Mar 20	0.0	1.0	154.74	3.77	4.05	0.75	1.21	0.30	0.80	0.12	178.64	112.04	2.0
Italy	Mar 11	Mar 16	0.0	0.0	-6094.77	4.16	2.79	0.50	1.00	0.53	0.46	0.53	935.34	1928.88	1.0
Norway	Mar 24	Mar 11	4.0	12.0	-151.02	4.04	3.46	0.41	1.07	0.13	0.68	0.27	353.40	486.72	2.0
Spain	Mar 14	Mar 08	1.0	1.0	-55.73	3.94	3.62	0.61	1.11	0.07	0.73	0.53	898.03	897.61	2.0
Sweden	Mar 18	Mar 10	4.0	7.0	-258.97	4.02	3.50	0.42	1.06	0.11	0.64	0.25	386.21	494.37	2.0
Switzerland	Mar 20	Mar 20	3.0	9.0	-105.13	3.95	3.74	0.62	1.11	0.18	0.47	0.21	203.22	230.43	2.0
United Kingdom	Mar 24	Mar 18	9.0	9.0	12.13	3.98	3.82	0.54	1.15	0.21	0.83	0.39	268.76	260.68	2.0
Wuhan, China	Jan 23	Feb 03	2.0	3.0	27.03	3.73	3.63	0.61	1.15	0.28	0.18	0.35	597.87	561.16	2.0

Table 2: Parameter estimates for different regions. See Eq. (1) for model parameters. All estimates are posterior medians. 75% and 95% credible intervals given only for τ, in days. τ^* is the official last NPI date, see Table 1.

Late effective start of NPIs. In both Wuhan, China, and in Italy we find that our estimated effective start of NPI $\hat{\tau}$ is significantly later than the official date τ^* (Figure 1).

In Italy, the first case was officially confirmed on Feb 21. School closures were implemented on Mar 5[6], a lockdown was declared in Northern Italy on Mar 8, with social distancing implemented in the rest of the country, and the lockdown was extended to the entire nation on Mar 11[8]. That is, the first and last official dates are Mar 8 and Mar 11. However, we estimate the effective date $\hat{\tau}$ at Mar 16 (±0.47 days 95% CI ; Figure 2). Similarly, in Wuhan, China, a lockdown was ordered on Jan 23[11], but we estimate the effective start of NPIs to be several days layer at Feb 2 (±2.85 days 95% CI Figure 2).

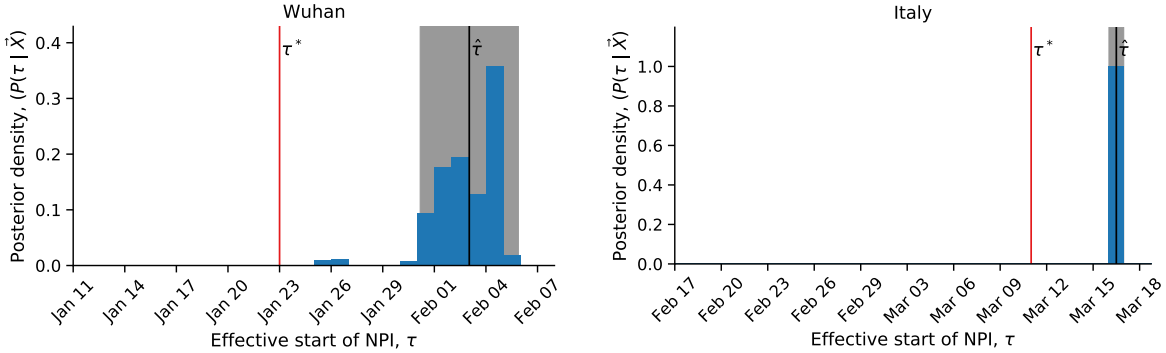

Figure 2: Late effect of non-pharmaceutical interventions in Italy and Wuhan, China. Posterior distribution of τ, the effective start date of NPI, is shown as a histogram of MCMC samples. Red line shows the official last NPI date τ^*. Black line shows the estimated $\hat{\tau}$. Shaded area shows a 95% credible interval (area in which $P(|\tau - \hat{\tau}| \mid \mathbf{X}) = 0.95$).

Early effective start of NPIs. In contrast, in some regions we estimate an effective start of NPIs $\hat{\tau}$ that is *earlier* then the official date τ^* (Figure 1). In Spain, social distancing was encouraged starting on Mar 8[6], but mass gatherings still occurred on Mar 8, including a march of 120,000 people for the International Women's Day, and a football match between Real Betis and Real Madrid (2:1) with a crowd of 50,965 in Seville. A national lockdown was only announced on Mar 14[6]. Nevertheless, we estimate the effective start of NPI $\hat{\tau}$ on Mar 8 or 9 (±1.08 95%CI), rather than Mar 14 (Figure 3).

Similarly, in France we estimate the effective start of NPIs $\hat{\tau}$ on Mar 8 or Mar 9 (±6.27 days 95% CI, Figure 3). Although the credible interval is wider compared to Spain, spanning from Mar 2 to Mar 15, the official lockdown start at Mar 17 is later still, and even the earliest NPI, banning of public events, only started on Mar 13[6].

Interestingly, the effective start of NPIs $\hat{\tau}$ in both France and Spain is estimated at Mar 8, although the official NPI dates differ significantly: the first NPI in France is only one day before the last NPI in Spain. The number of daily cases was similar in both countries until Mar 8, but diverged by Mar 13, reaching significantly higher numbers in Spain (Figure S3). This may suggest that correlation exist between effective start of NPIs due to global or international events.

The exception that proves the rule. We find one case in which the official and effective dates match: Switzerland ordered a national lockdown on Mar 20, after banning public evens and closing schools on Mar 13 and 14[6]. Indeed, the posterior median $\hat{\tau}$ is Mar 20 (±8.46 days 95% CI), and the posterior distribution shows two density peaks: a smaller one between Mar 10 and Mar 14, and a bigger one between Mar 17 and Mar 22 (Figure S4). It's also worth mentioning that Switzerland was the first to mandate self isolation of confirmed cases[6].

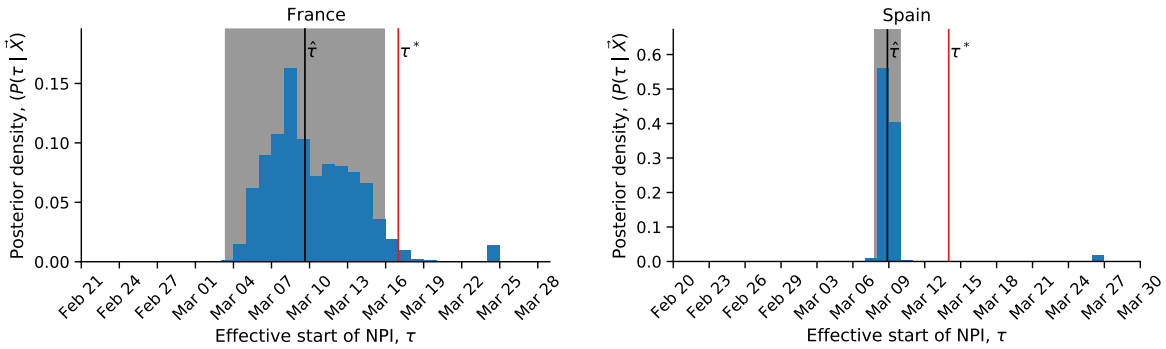

Figure 3: Early effect of non-pharmaceutical interventions in France and Spain. Posterior distribution of τ, the effective start date of NPI, is shown as a histogram of MCMC samples. Red line shows the official last NPI date τ^*. Black line shows the estimated $\hat{\tau}$. Shaded area shows a 95% credible interval (area in which $P(|\tau - \hat{\tau}| \mid \mathbf{X}) = 0.95$).

Effect of late and early effect of NPIs on real-time assessment. The success of non-pharmaceutical interventions is assessed by health officials using various metrics, such as the decline in the growth rate of daily cases. These assessments are made a specific number of days after the intervention began, to accommodate for the expected serial interval[3] (i.e. time between successive cases in a chain of transmission), which is estimated at about 4-7 days[8].

However, a significant difference between the beginning of the intervention and the effective change in transmission rates can invalidate assessments that assume a serial interval of 4-7 days and neglect the late or early population response to the NPI. This is illustrated in Figure 4 using data and parameters from Italy. Here, a lockdown is officially ordered on Mar 10 (τ^*), but its late effect on the transmission dynamics starts on Mar 16 ($\hat{\tau}$). If health officials assume the dynamics to immediately change at τ^*, they will expect the number of cases be within the red lines (posterior predictions assuming $\tau = \tau^*$). This leads to a significant underestimation, which might be interpreted by officials as ineffectiveness of NPIs, leading to further escalations. However, the number of cases will actually follow the blue lines (posterior predictions using $\tau = \hat{\tau}$), which corresponds well to the real data.

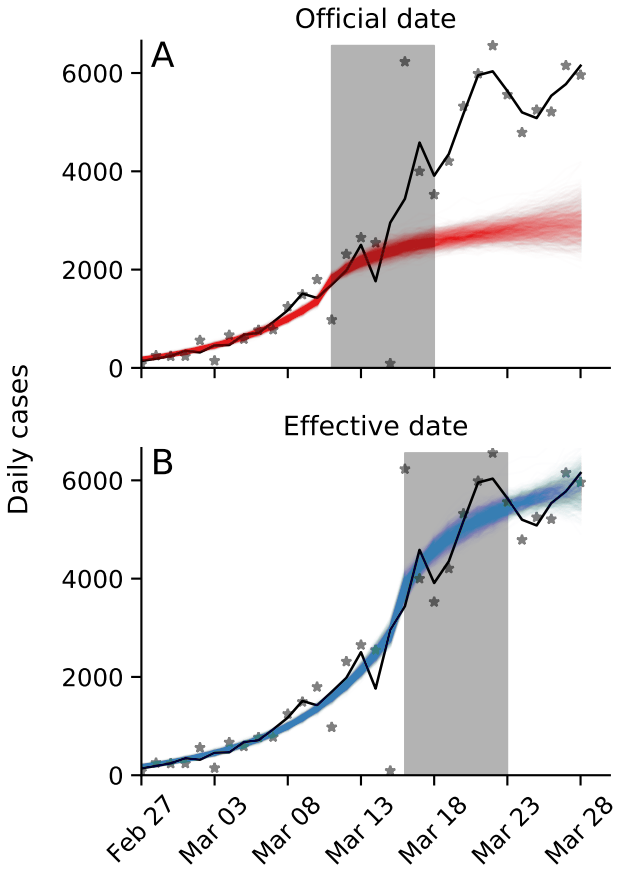

Figure 4: Late effective start of NPIs leads to under-estimation of daily confirmed cases. Real number of daily cases in Italy in black (markers: data, line: time moving average). Model posterior predictions are shown as colored lines (1,000 draws from the posterior distribution). Shaded box illustrates a serial interval of seven days. **(A)** Using the official date τ^* for the start of the NPI, the model under-estimates the number of cases seven days after the start of the NPI. **(B)** Using the effective date $\hat{\tau}$ for the start of the NPI, the model correctly estimates the number of cases seven days after the start of the NPI. Here, model parameters are estimates for Italy (Table 2).

Discussion

We have estimated the effective start date of NPIs in several geographical regions using an SEIR epidemiological model and an MCMC parameter estimation framework. We find examples of both late and early effect of NPIs (Figure 1).

For example, in Italy and Wuhan, China, the effective start of the lockdowns seems to have occurred more than five days after the official date (Figure 2). This difference might be explained by low compliance: In Italy, for example, the government intention to lockdown Northern provinces leaked to the public, resulting in people leaving those provinces[8]. Late effect of NPIs might also be due to the time required by both the government and the citizens to organize for a lockdown, and for the new guidelines to diffuse in the population.

In contrast, in most investigated countries (e.g., Spain and France), we infer reduced transmission rates even before official lockdowns were implemented (Figure 3). This early response might be due to adoption of social distancing and similar behavioral adaptations in parts of the population, maybe in response to increased risk perception due to domestic or international COVID-19-related reports. This finding may also suggest that severe NPIs, such as lockdowns, were unnecessary, and that less extreme measures adopted by the population could have been sufficient for epidemic control. These less

extreme measures may have been implemented due to government recommendations, media coverage, and social networks, rather than official NPIs. check if this is true Indeed, the evidence supports a change in transmission dynamics (i.e. a model with τ) even for Sweden, in which a lockdown was not implemented, suggesting that lockdowns may not be necessary if other NPIs are adopted early enough during the outbreak[3] (Sweden banned public events on Mar 12, encouraged social distancing on Mar 16, and closed schools on Mar 18[6].)

Attempts to asses the effect of NPIs[3,6] generally assume a seven days delay between the implementation of the intervention and the observable change in dynamics, due to the characteristic serial interval of COVID-19[8]. However, the late and early effects we have estimated can confuse these assessments and lead to wrong conclusions about the effects of NPIs (Figure 4).

We have found that the evidence supports a model in which the parameters change at a specific time point τ over a model without such a change-point. It may be interesting to investigate if the evidence favors a model with *two* change-points, rather than one. Two such change-points could reflect escalating NPIs (e.g. school closures followed by lockdowns), or a mix of NPIs and other events, such as weather, or domestic and international events that affect risk perception.

As several countries (e.g. Austria, Israel) begin to relieve lockdowns and ease restrictions, we expect similar delays and advances to occur: in some countries people will begin to behave as if restrictions were eased even before the official date, and in some countries people will continue to self-restrict even after restrictions are officially removed.

Conclusions. We have estimated the effective start date of NPIs and found that they often differ from the official dates. Our results highlight the complex interaction between personal, regional, and global determinants of behavioral response to infectious disease. Therefore, we emphasize the need to further study variability in compliance and behavior over both time and space. This can be accomplished both by surveying differences in compliance within and between populations[2], and by incorporating specific behavioral models into epidemiological models[1,5,15].

Acknowledgements

We thank Lilach Hadany and Oren Kolodny for discussions and comments. This work was supported in part by the Israel Science Foundation 552/19 and 1399/17.

References

[1] Arthur, R. F., Jones, J. H., Bonds, M. H. and Feldman, M. W. 2020, 'Complex dynamics induced by delayed adaptive behavior during outbreaks', *bioRxiv* pp. 1–23.

[2] Atchison, C. J., Bowman, L., Vrinten, C., Redd, R., Pristera, P., Eaton, J. W. and Ward, H. 2020, 'Perceptions and behavioural responses of the general public during the COVID-19 pandemic: A cross-sectional survey of UK Adults', *medRxiv* p. 2020.04.01.20050039.

[3] Banholzer, N., Weenen, E. V., Kratzwald, B. and Seeliger, A. 2020, 'The estimated impact of non-pharmaceutical interventions on documented cases of COVID-19 : A cross-country analysis', *medRxiv* .

[4] Dunn, A. G., Leask, J., Zhou, X., Mandl, K. D. and Coiera, E. 2015, 'Associations between exposure to and expression of negative opinions about human papillomavirus vaccines on social media: An observational study', *J. Med. Internet Res.* **17**(6), e144.

[5] Fenichela, E. P., Castillo-Chavezb, C., Ceddiac, M. G., Chowellb, G., Gonzalez Parrae, P. A., Hickling, G. J., Holloway, G., Horan, R., Morin, B., Perrings, C., Springborn, M., Velazquez, L. and Villalobos, C. 2011, 'Adaptive human behavior in epidemiological models', *Proc. Natl. Acad. Sci. U. S. A.* **108**(15), 6306–6311.

[6] Flaxman, S., Mishra, S., Gandy, A., Unwin, J. T., Coupland, H., Mellan, T. A., Zhu, H., Berah, T., Eaton, J. W., Guzman, P. N. P., Schmit, N., Cilloni, L., Ainslie, K. E. C., Baguelin, M., Blake, I., Boonyasiri, A., Boyd, O., Cattarino, L., Ciavarella, C., Cooper, L., Cucunubá, Z., Cuomo-Dannenburg, G., Dighe, A., Djaafara, B., Dorigatti, I., Van Elsland, S., Fitzjohn, R., Fu, H., Gaythorpe, K., Geidelberg, L., Grassly, N., Green, W., Hallett, T., Hamlet, A., Hinsley, W., Jeffrey, B., Jorgensen, D., Knock, E., Laydon, D., Nedjati-Gilani, G., Nouvellet, P., Parag, K., Siveroni, I., Thompson, H., Verity, R., Volz, E., Gt Walker, P., Walters, C., Wang, H., Wang, Y., Watson, O., Xi, X., Winskill, P., Whittaker, C., Ghani, A., Donnelly, C. A., Riley, S., Okell, L. C., Vollmer, M. A. C., Ferguson, N. M. and Bhatt, S. 2020, 'Estimating the number of infections and the impact of non-pharmaceutical interventions on COVID-19 in 11 European countries', *Imp. Coll. London* (March), 1–35.
URL: *https://doi.org/10.25561/77731*

[7] Foreman-Mackey, D., Hogg, D. W., Lang, D. and Goodman, J. 2013, 'emcee : The MCMC Hammer ', *Publ. Astron. Soc. Pacific* **125**(925), 306–312.

[8] Gatto, M., Bertuzzo, E., Mari, L., Miccoli, S., Carraro, L., Casagrandi, R. and Rinaldo, A. 2020, 'Spread and dynamics of the COVID-19 epidemic in Italy: Effects of emergency containment measures', *Proc. Natl. Acad. Sci.* p. 202004978.
URL: *http://www.pnas.org/lookup/doi/10.1073/pnas.2004978*

[9] Goodman, J. and Weare, J. 2010, 'Ensemble Samplers With Affine Invariance', *Commun. Appl. Math. Comput. Sci.* **5**(1), 65–80.

[10] Kaufman, M. R., Cornish, F., Zimmerman, R. S. and Johnson, B. T. 2014, 'Health behavior change models for HIV prevention and AIDS care: Practical recommendations for a multilevel approach', *J. Acquir. Immune Defic. Syndr.* **66**(SUPPL.3), 250–258.

[11] Li, R., Pei, S., Chen, B., Song, Y., Zhang, T., Yang, W. and Shaman, J. 2020, 'Substantial undocumented infection facilitates the rapid dissemination of novel coronavirus (SARS-CoV2)', *Science (80-.).* p. eabb3221.
URL: *https://www.sciencemag.org/lookup/doi/10.1126/scienc*

[12] Pei, S. and Shaman, J. 2020, 'Initial Simulation of SARS-CoV2 Spread and Intervention Effects in the Continental US', *medRxiv* p. 2020.03.21.20040303.
URL: *http://medrxiv.org/content/early/2020/03/23/2020.03.2*

[13] Smith, L. E., Mottershaw, A. L., Egan, M., Waller, J., Marteau, T. M. and Rubin, G. J. 2020, 'The impact of believing you have had COVID-19 on behaviour : Cross-sectional survey', *medRxiv* pp. 1–20.

[14] Spiegelhalter, D. J., Best, N. G., Carlin, B. P. and Van Der Linde, A. 2002, 'Bayesian measures of model complexity and fit', *J. R. Stat. Soc. Ser. B Stat. Methodol.* **64**(4), 583–616.

[15] Walters, C. E. and Kendal, J. R. 2013, 'An SIS model for cultural trait transmission with conformity bias', *Theor. Popul. Biol.* **90**, 56–63.
URL: *http://dx.doi.org/10.1016/j.tpb.2013.09.010*

[16] Wiyeh, A. B., Cooper, S., Nnaji, C. A. and Wiysonge, C. S. 2018, 'Vaccine hesitancy âĂŸoutbreaks': using epidemiological modeling of the spread of ideas to understand the effects of vaccine related events on vaccine hesitancy', *Expert Rev. Vaccines* **17**(12), 1063–1070. **URL:** *https://doi.org/10.1080/14760584.2018.1549994*

[17] Zipfel, C. M. and Bansal, S. 2020, 'Assessing the interactions between COVID-19 and influenza in the United States', *medRxiv* (February), 1–13. **URL:** *https://doi.org/10.1101/2020.03.30.20047993*

Supplementary Material

Austria

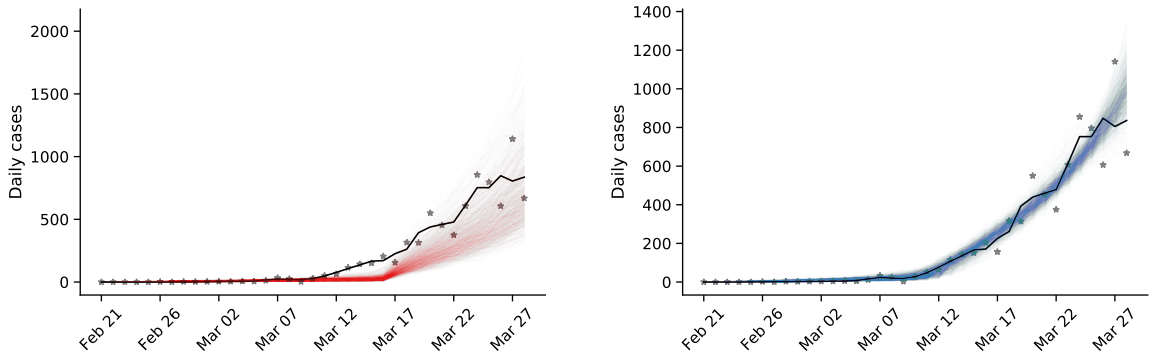

Belgium

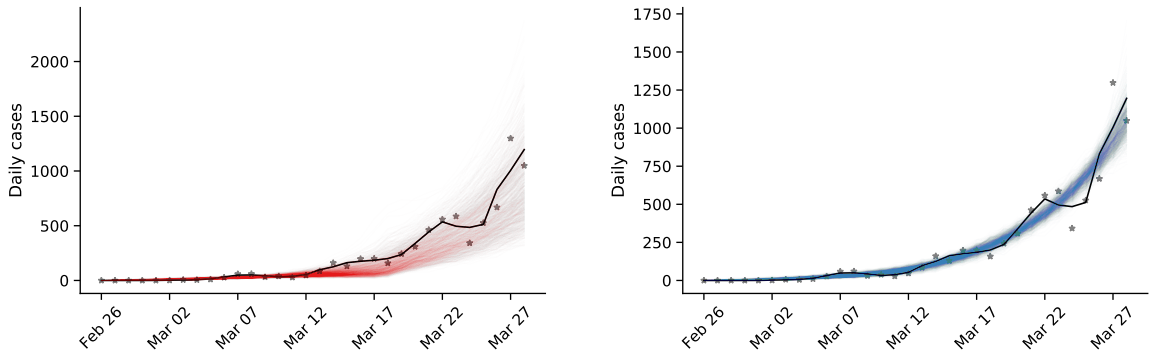

Denmark

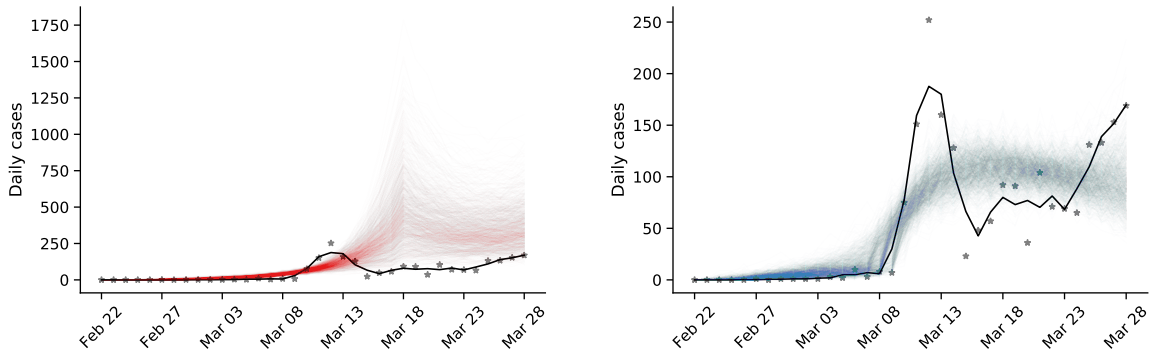

France

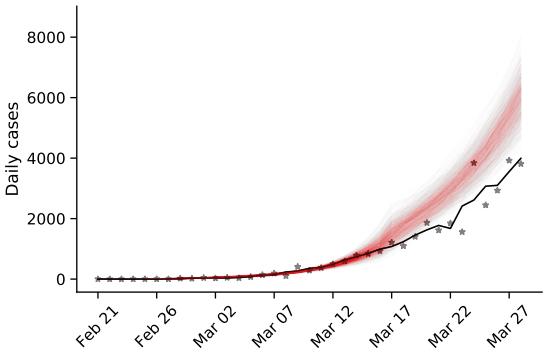

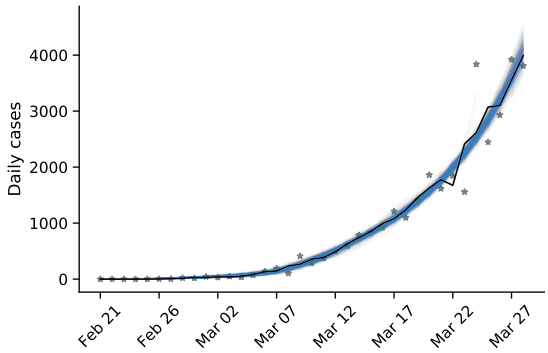

Germany

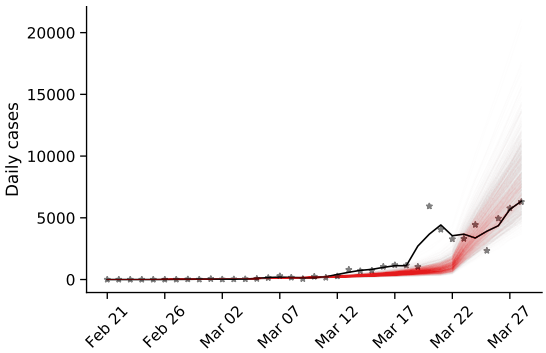

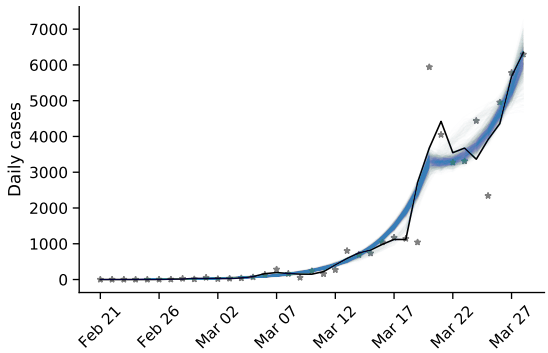

Italy

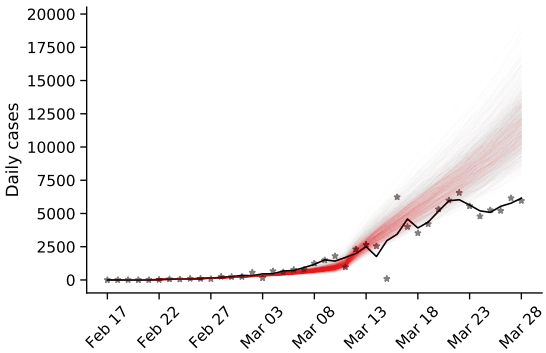

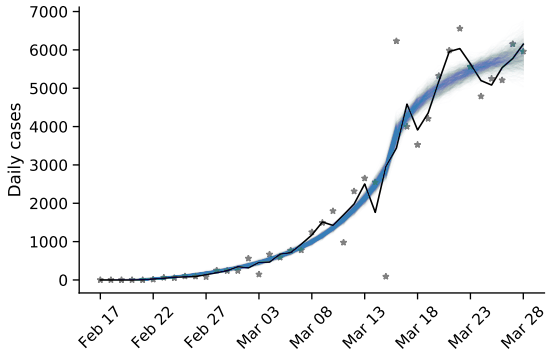

Norway

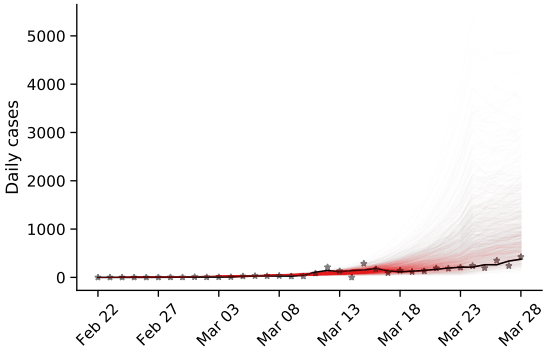

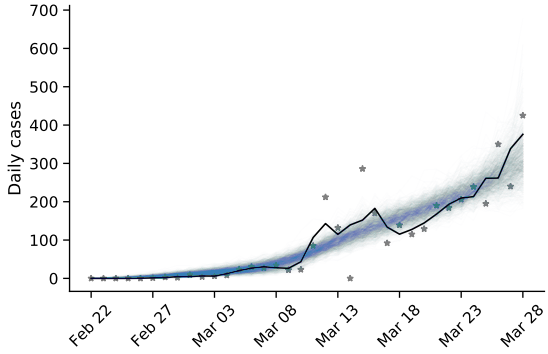

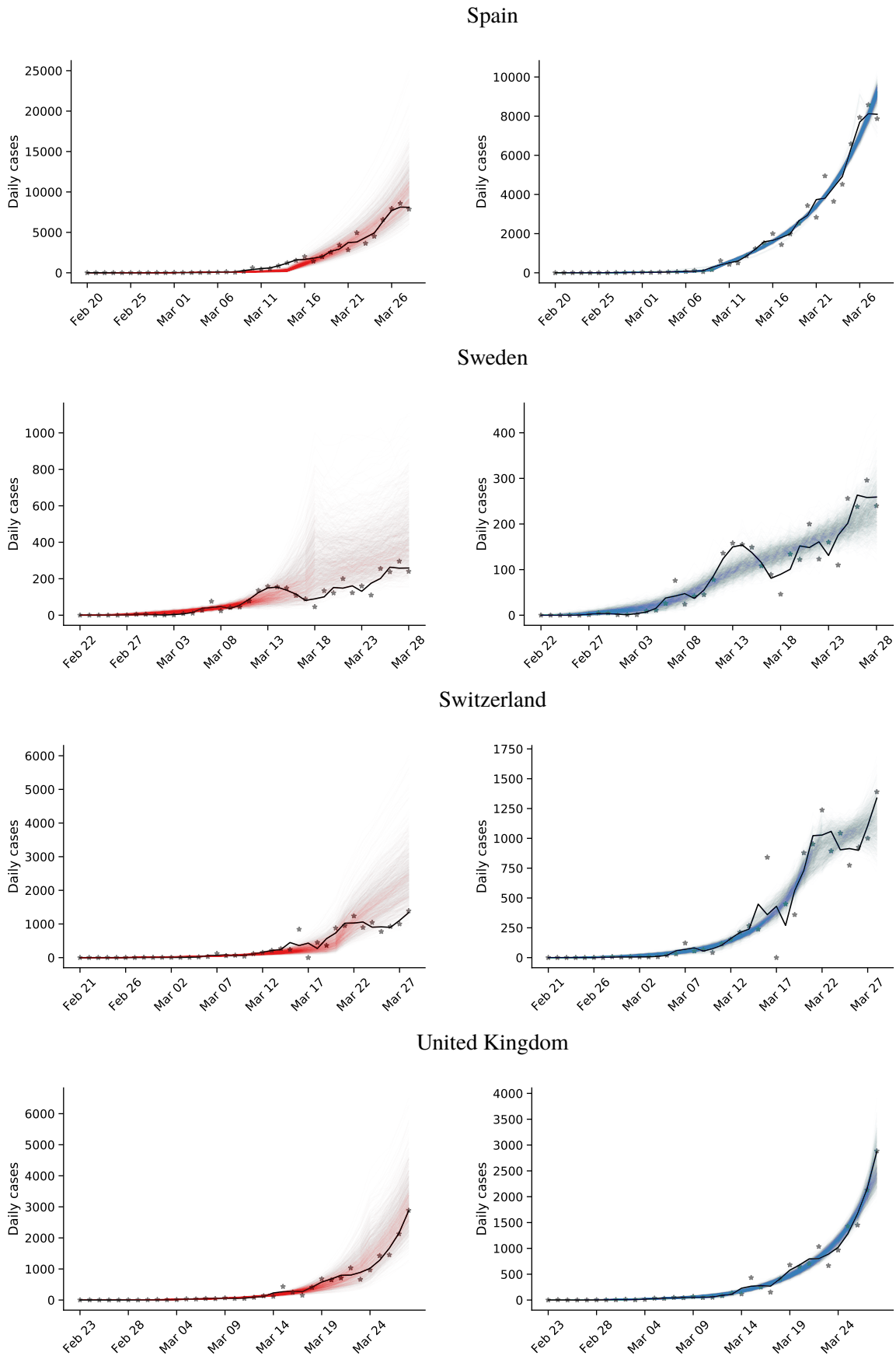

Figure S1. Posterior prediction check plots Markers represent data (**X**). Black line represent a smoothing of the data points using a Savitzky-Golay filter. Color lines represent posterior predictions from a model with fixed τ, in red, and free τ, in blue. These predictions are made by drawing 1,000 samples from the parameter posterior distribution and then generating a daily case count using the SEIR model in Eq. (1). Note the differences in the y-axis scale.

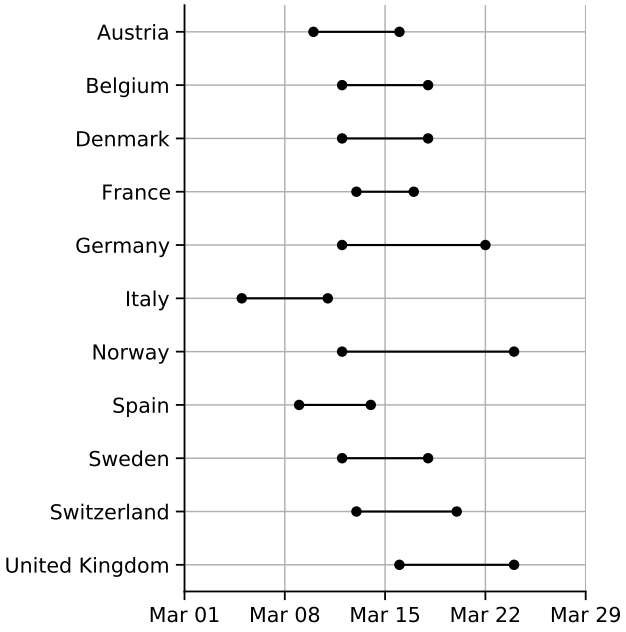

Figure S2: Official start of non-pharmaceutical interventions. See Table 1 for more details. Wuhan, China is not shown.

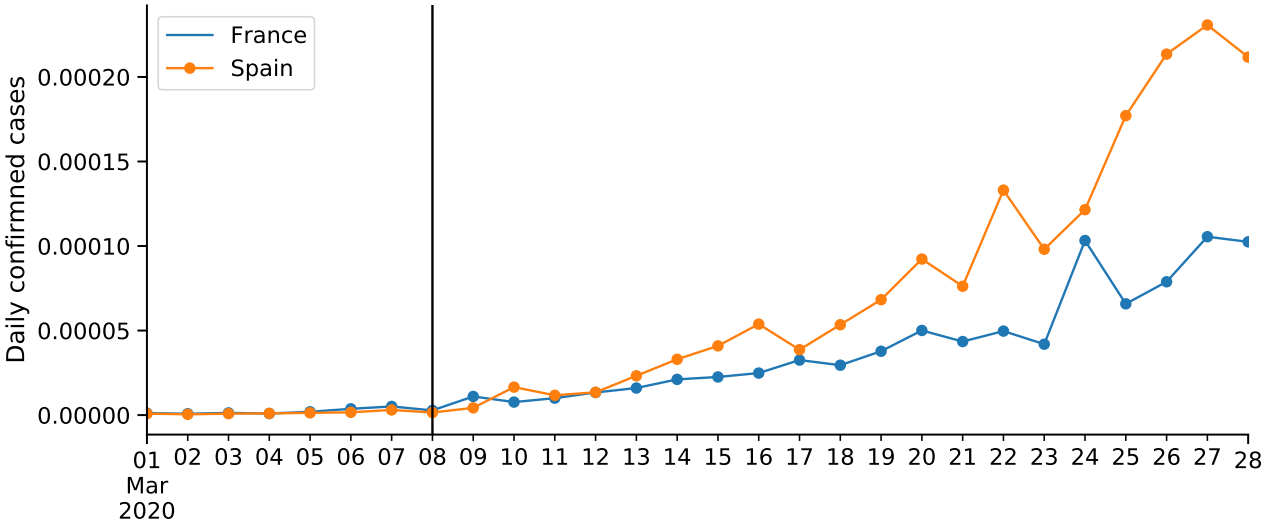

Figure S3: COVID-19 confirmed cases in France and Spain. Number of cases proportional to population size (as of 2018). Vertical line shows Mar 8, the effective start of NPIs $\hat{\tau}$ in both countries.

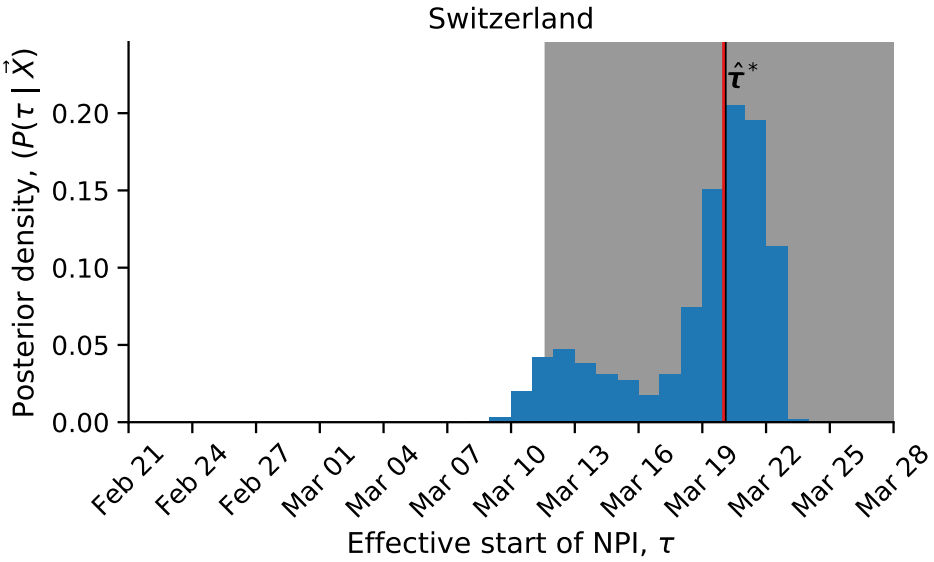

Figure S4: Late effect of non-pharmaceutical interventions in Switzerland. Posterior distribution of τ, the effective start date of NPI, is shown as a histogram of MCMC samples. Red line shows the official last NPI date τ^*. Black line shows the estimated $\hat{\tau}$. Shaded area shows a 95% credible interval (area in which $P(|\tau - \hat{\tau}| \mid \mathbf{X}) = 0.95$).